Onset and Progression of Disease in Nonhuman Primates With PDE6C Cone Disorder

Monica Ardon,[1] Lily Nguyen,[1] Rui Chen,[2,3] Jeffrey Rogers,[2] Tim Stout,[4] Sara Thomasy,[1,5,6] and Ala Moshiri[1]

[1]Department of Ophthalmology & Vision Science, School of Medicine, University of California Davis, Sacramento, California, United States
[2]Human Genome Sequencing Center and Department of Molecular and Human Genetics, Baylor College of Medicine, Houston, Texas, United States
[3]Department of Biochemistry and Molecular Biology, Baylor College of Medicine, Houston, Texas, United States
[4]Department of Ophthalmology, Cullen Eye Institute, Baylor College of Medicine, Houston, Texas, United States
[5]Department of Surgical and Radiological Sciences, School of Veterinary Medicine, University of California-Davis, Davis, California, United States
[6]California National Primate Research Center, Davis, California, United States

Correspondence: Ala Moshiri, UC Davis Eye Center, Ernest E. Tschannen Eye Institute, 4860 Y Street, Sacramento, CA 95817, USA; amoshiri@ucdavis.edu.

Received: May 24, 2024
Accepted: November 19, 2024
Published: December 6, 2024

Citation: Ardon M, Nguyen L, Chen R, et al. Onset and progression of disease in nonhuman primates with PDE6C cone disorder. *Invest Ophthalmol Vis Sci.* 2024;65(14):16. https://doi.org/10.1167/iovs.65.14.16

Purpose. The California National Primate Research Center contains a colony of rhesus macaques with a homozygous missense mutation in *PDE6C* (R565Q) which causes a cone disorder similar to *PDE6C* achromatopsia in humans. The purposes of this study are to characterize the phenotype in *PDE6C* macaques in detail to determine the onset of the cone phenotype, the degree to which the phenotype progresses, if heterozygote animals have an intermediate phenotype, and if rod photoreceptor function declines over time.

Methods. We analyzed spectral-domain optical coherence tomography (SD-OCT), fundus autofluorescence (FAF), and electroretinography (ERG) data from 102 eyes of 51 macaques (aged 0.25 to 16 years). Measurements of retinal layers as well as cone and rod function over time were quantitatively compared.

Results. Homozygotes as young as 3 months postnatal showed absent cone responses on electroretinogram. Infant homozygotes had reduced foveal outer nuclear layer (ONL) thickness compared with wildtype infants ($P < 0.0001$). Over 4 years of study, no consistent changes in retinal layer thicknesses were found within 5 adult homozygotes. However, comparisons between infants and adults revealed reductions in foveal ONL thickness suggesting that cone cells slowly degenerate as homozygotes age. The oldest homozygote (11 years) had reduced rod responses. Heterozygotes could not be distinguished from wildtypes in any parameters.

Conclusions. These data suggest that, like humans, macaque *PDE6C* heterozygotes are normal, and homozygote primates have absent cone function and reduced foveal ONL thickness from infancy. Cone photoreceptors probably degenerate over time and macular atrophy can occur. Rod photoreceptor function may wane in late stages.

Keywords: genetic diseases, ophthalmology, PDE6C, achromatopsia (ACHM), photoreceptors

Achromatopsia (ACHM) affects 1 in 30,000 people in the United States and has no current treatment.[1–3] Individuals with ACHM are usually legally blind (visual acuity $\leq$ 20/200), suffer from photophobia, have complete color blindness, and absent cone-mediated electroretinographic (ERG) amplitudes.[1,2] Currently, there are 6 known genes that have been linked to ACHM: *CNGA3*, *CNGB3*, *GNAT2*, *ATF6*, *PDE6C*, and *PDE6H*.[4–6] *PDE6C* encodes the catalytic alpha subunit of the cone photoreceptor phosphodiesterase 6.[4,7,8] Mutations in *PDE6C* are rare and its prevalence only accounts for 2.4% in a cohort of 1074 independent ACHM families.[5] Due to the low prevalence of individuals with *PDE6C*-ACHM and the lack of large animal models of *PED6C*-ACHM, no effective therapies are available.[8]

In humans, *PDE6C*-ACHM is seen from infancy where it presents with photophobia, nystagmus, absent color discrimination, and poor visual acuity.[4,8] Variants of *PDE6C*-ACHM have been reported to cause both complete and incomplete ACHM, cone dystrophy, and cone-rod dystrophy.[4] This is further confirmed in ERG findings where there is absent cone function and rod dysfunction is occasionally observed.[8,9] Another feature of *PDE6C*-ACHM is progressive cone cell loss beginning in early childhood with progressive retinal thinning as patients age.[10–12] This observation contrasts with other forms of ACHM, which are essentially stationary with cell loss and retinal thinning occurring extremely slowly over the course of life.[13]

In our previous 2019 study, we identified 4 related rhesus macaques (*Macaca mulatta*) at the California National Primate Research Center with suspected visual impairment through behavioral observations.[8] Genetic sequencing confirmed a homozygous R565Q missense mutation in the catalytic domain of *PDE6C*.[8] These primates exhibit a clinical phenotype similar to human *PDE6C*-ACHM where both species exhibit completely absent cone function with a normal rod response by ERG.[8] However, in some cases, it has been reported that rod response can decrease with age in humans.[14,15] These macaques also demonstrated thinning of the foveal outer nuclear layer (ONL) with altered foveal pigmentation which could be due to the higher visibility of underlying RPE melanin.[8] The oldest homozygote (11 years old) demonstrated reduced rod response when compared to the next oldest homozygote (3 years 9 months of age)[8] which suggested age-related rod functional decline. No infant homozygotes were available at the time so we could not confirm if the ACHM phenotype presents in infancy as it does in humans.

After initiating our selective breeding program to obtain homozygous infants, we sought to quantify the phenotype in detail during infancy to determine onset of the phenotype. Furthermore, we also assessed the degree to which the phenotype progresses with age, if heterozygote animals have an intermediate phenotype, and if rod photoreceptor function is affected.

Materials and Methods

Study Animals

Data were collected from 102 eyes of 51 rhesus macaques (*Macaca mulatta*) between 0.25 and 16 years of age. Primates were grouped based on age and genotype. Primates were considered infants if they were less than 12 months of age and were considered adults if they were over 3 years of age. We included a total of 29 infants; there were 13 male primates and 16 female primates. Mean ± standard deviation (SD) age of the primates was 5.28 ± 2.33 months (range = 2–11 months and median = 5 months). There was a total of 22 adults; there were 5 male primates and 17 female primates. Mean ± SD age of the primates was 6.73 ± 3.44 years (range = 3–16 years and median = 6 years). Demographics and genetics are summarized in the Table. A more detailed description of demographics, genetics, and imaging done for each primate can be found in Supplementary Table S1. All rhesus macaques were born and sustained at the California National Primate Research Center (CNPRC). The CNPRC is accredited by the Association for Assessment and Accreditation of Laboratory Animal Care (AAALAC) International. The study was approved by and performed according to the Institutional Animal Care and Use Committee (IACUC protocol #22508) of the University of California – Davis and the National Institutes of Health (NIH) *Guide for the Care and Use of Laboratory Animals,* respectively. Guidelines outlined in the Association for Research in Vision and Ophthalmology Statement for the Use of Animals in Ophthalmic and Vision Research were followed. Rhesus macaques were sedated with ketamine hydrochloride (5–30 mg/kg), midazolam (0.1 mg/kg), and dexmedetomidine (0.05–0.07515 mg/kg) intramuscularly for examinations and were medically monitored by a CNPRC veterinarian and trained technician.

Table. Demographics and Genetics Data

	Infant (2–11 Months Old)			Adult (3–6 Years Old)		
	Male	Female	Total	Male	Female	Total
Wildtype	3	3	6	2	6	8
Homozygous	3	9	12	1	4	5
Heterozygous	7	4	11	2	7	9

Table shows number of primates in each age, sex, and genotype group.

Electroretinography and Ophthalmic Imaging

While sedated, the animals' eyes were dilated and then dark adapted for 30 minutes in preparation for ERG acquisition. The RETevet device (LKC Technologies, Inc., Gaithersburg, MD, USA) was used to perform ERG to obtain implicit time (ms) and amplitude (μV) for each eye at all examinations. Scotopic ERG testing consisted of flash stimuli at 0.01, 3.0, and 10.0 cd·s/m^2 in the dark-adapted state. Afterward, the primates were light-adapted for 10 minutes and photopic ERGs captured using flash stimuli of 3.0 cd·s/m^2 intensity; a 30 hertz (Hz) photopic flicker was also obtained at that light intensity. Measurements were recorded and presented using the manufacturer's software.

Spectral-domain optical coherence tomography (SD-OCT) images were obtained for quantitative measurements of retinal layers using Heidelberg Explorer software (version 1.8.6.0; Heidelberg Engineering, Heidelberg, Germany). For foveal measurements, SD-OCT images were selected based on where the fovea displayed the greatest depth. Images were then calibrated on Image J (National Institutes of Health, Bethesda, MD, USA) based on the manufacturer's scale. We assessed retinal layer thickness at 1 mm both nasal and temporal to the fovea and at the foveal center. Total retinal thickness for nasal and temporal measurements were measured from the internal limiting membrane up to but not including the RPE. All thickness measurements were conducted by two observers (authors M.A. and L.N.) using Image J and averaged. Measurements for both eyes of each animal were averaged based on the anatomic location. Last, macaques were photographed to obtain color fundus photography images using a Canon CF-1 Retinal Camera with a 50 degree wide-angle lens.

Statistical Analysis

Measurements for both eyes of each animal were averaged.

Quantitative comparisons of ERG amplitudes (Fig. 1A) were performed using ordinary 1-way ANOVA to determine any significant variation in cone photoreceptor function among the three infant macaque genotypes. Dunnett's multiple comparisons test was used for post hoc comparisons to account for multiple testing. Quantitative comparisons of ERG amplitudes (Fig. 1B) were compared using 2-way ANOVA to determine if age and genotype had an effect on cone photoreceptor response. Foveal retinal layer thickness (Figs. 2A, 3A) were compared using 2-way ANOVA to ascertain any significant interactions between genotype and retinal layer thickness. Analysis was followed up with Tukey's multiple comparisons test in Figure 1B and Dunnett's multiple comparisons test in Figures 2A and 3A. Similarly, 2-way ANOVA was used to determine any significant interac-

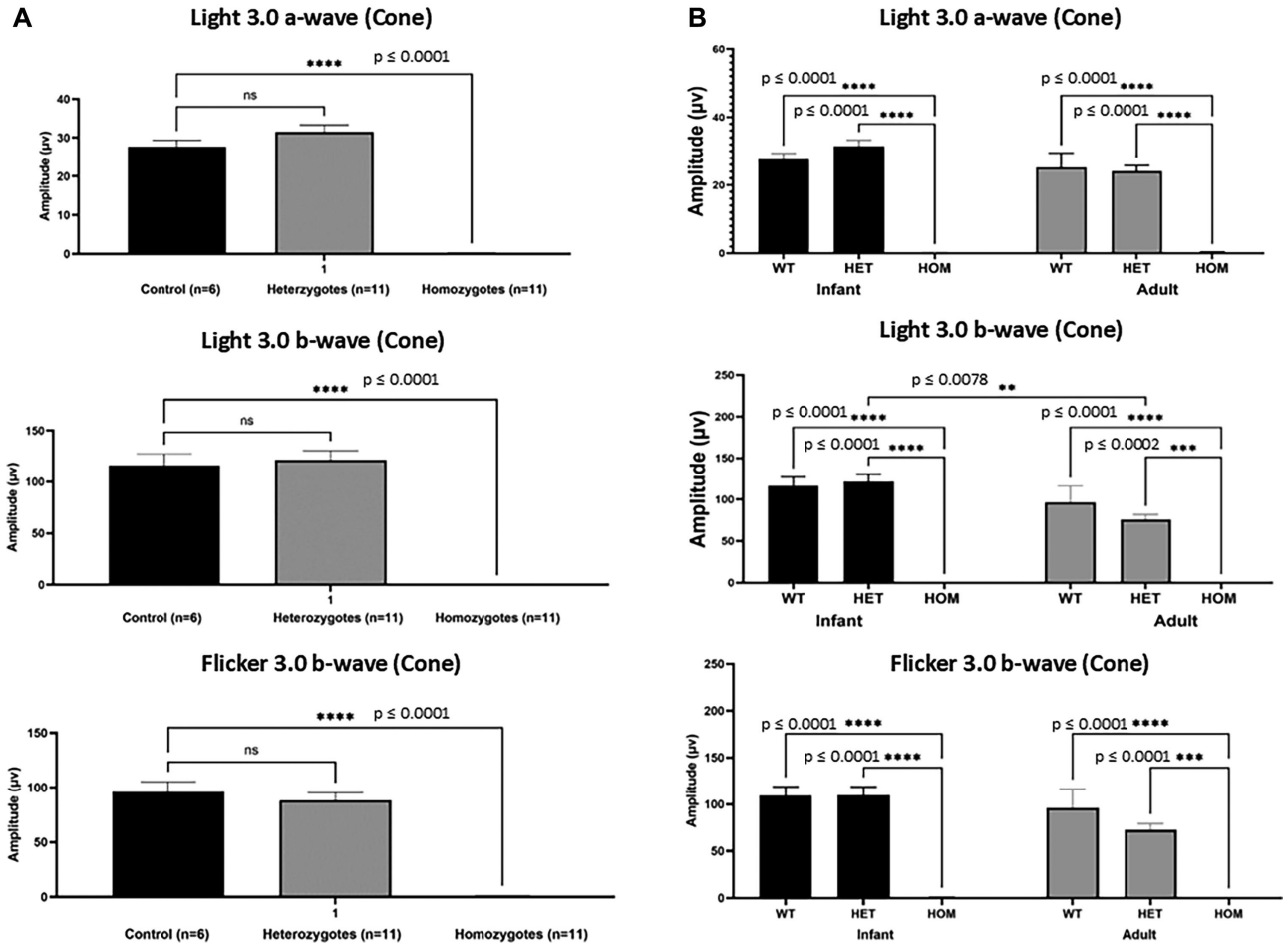

Figure 1. Homozygous primates were shown to have nearly undetectable cone responses beginning from infancy. (**A**) Mean ± SEM ERG amplitudes (μV: microvolts) of both a- and b-waves from infant wildtype ($n = 6$), homozygotes ($n = 11$), and heterozygotes ($n = 11$) macaques was quantified and graphically depicted. Under light adapted conditions, a single flash 3.0 cd•s/m^2 stimulus, and a flicker (30 Hz) with the same stimulus resulted in nearly undetectable responses in homozygous macaques. Ordinary 1-way ANOVA revealed a significant interaction between genotype and amplitude at all three stimuli, F (2, 25) = 167.7, $P < 0.0001$, F (2, 25) = 91.70, $P < 0.0001$, and F (2, 25) = 82.11, $P < 0.0001$, respectively. Further post hoc analysis revealed a significant decrease ($P < 0.0001$) in homozygote infants (0.01 ± 0.3) when compared to infant wildtype (27.63 ± 1.7). No statistical significance was found between infant wildtype and heterozygotes. (**B**) Under light adapted conditions, a single flash 3.0 cd•s/m^2 stimulus of both a- and b-waves from electroretinogram amplitudes (μV: microvolts) of wildtype ($n = 6$), heterozygote ($n = 11$), homozygotes ($n = 11$), infants (age range = 2–11 months) and wildtype ($n = 7$), heterozygote ($n = 9$), homozygote ($n = 5$) adult macaques (age range = 3–16 years old) of flicker 3.0 b-wave was quantified and graphically depicted were amplitudes are presented as mean ± SEM of ERG amplitudes. Graphs show undetectable responses in infant and adult homozygotes when compared to their wildtype age groups. No statistical significance was found between age matched wildtype and heterozygote animals. Two-way ANOVA did not reveal a significant interaction between age and amplitude, F (2, 43) = 1.752, $P = 0.1856$. But 2-way ANOVA did reveal significance among genotype, F (2, 43) = 62.16, $P < 0.0001$ and among amplitude, F (1, 43) = 7.744, $P = 0.0080$. Data are presented as mean ± SEM. Two-way ANOVA shows a significance among genotype is present, F (2, 43) = 107.7, $P < 0.0001$. Tukey's post hoc analysis shows significance between wildtype and homozygote infants ($P < 0.0001$) and between heterozygote and homozygote infants ($P < 0.0001$). Similar results are seen in adult primates between wildtype and homozygotes ($P < 0.0001$) and between heterozygote and homozygote adults ($P < 0.0001$). There appears to be a mild age-related reduction in light 3.0 b-wave amplitude between heterozygote infant (121.4 ± 9.2 μV) and adult (75.9 ± 5.9 μV) macaques ($P = 0.0078$).

tions between foveal retinal layer thickness and age (adult and infant homozygotes; Fig. 3B) and were followed up with the Holm-Šídák method. Multiple paired *t*-tests were used to determine if there was a significant change in foveal retinal layer thickness in the same adult homozygotes over the course of 4 years (Fig. 3C). In all cases, *P* values less than 0.05 were deemed significant. Mean ± SD values in Figure 4G were from data that were previously published from normal rhesus macaques in the CNPRC colony.[16] Detailed statistical tests and post hoc analysis including *F* and *P* values are included in Supplementary Table S2. Wild-type primates were used as the control group in all relevant comparisons.

Results

Cone Photoreceptor Dysfunction Begins Near Birth

Photopic full field ERGs were performed on infant primates. To evaluate cone-mediated responses in wildtype ($n = 6$), homozygotes ($n = 11$), and heterozygote ($n = 11$) infants at

Investigative Ophthalmology & Visual Science

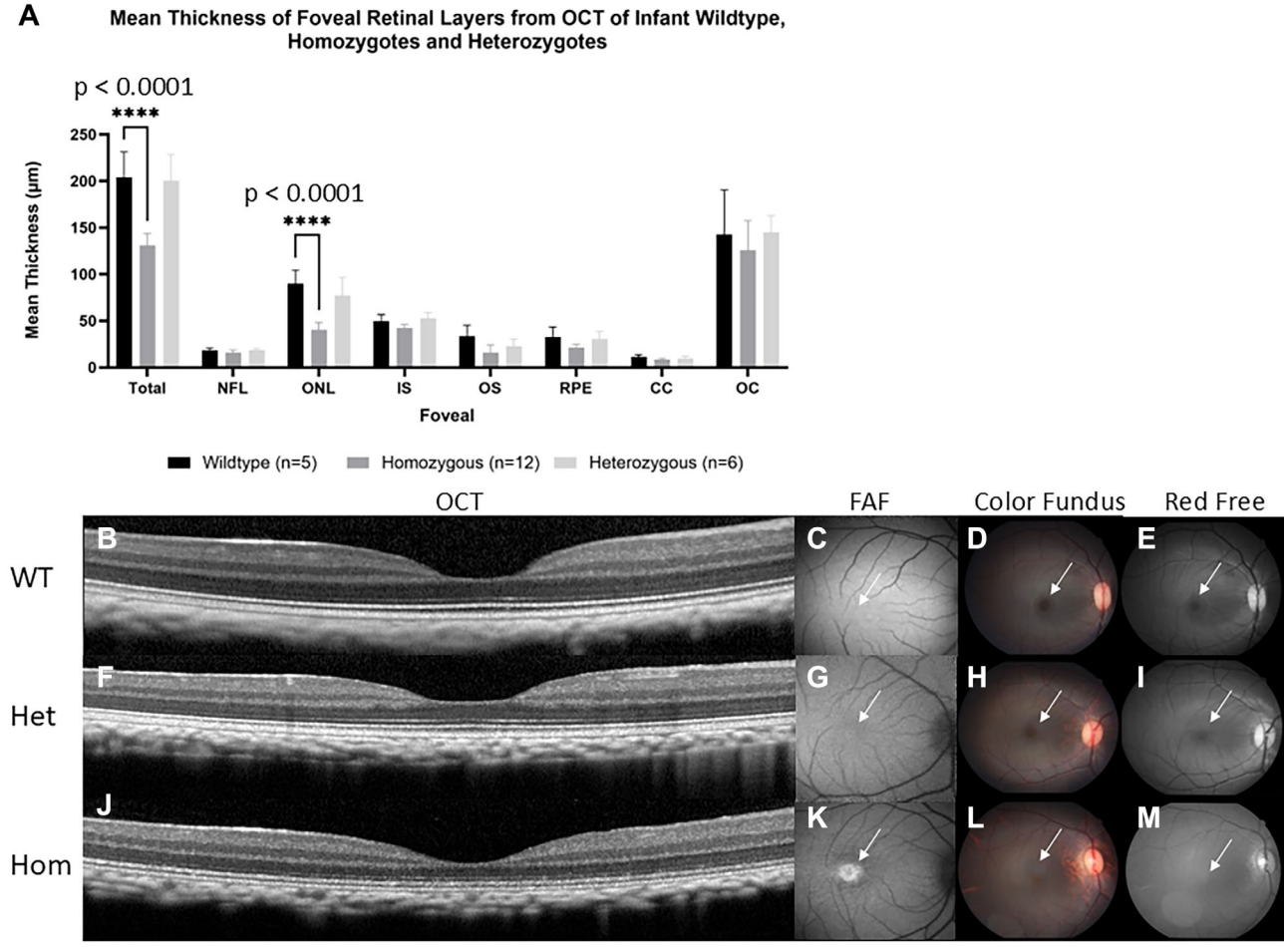

Figure 2. Homozygous infants were shown to have reduced foveal ONL thickness when compared to wildtype and heterozygous infant macaques. (**A**) Mean ± SEM thickness of retinal layers from spectral domain optical coherence tomography (SD-OCT) of infant wildtype (n = 5), homozygotes (n = 12), and heterozygotes (n = 6) macaques. Foveal ONL thinning is observed in homozygous infant rhesus macaques. Two-way ANOVA revealed a significant interaction between genotype and retinal layer thickness at total foveal thickness and at foveal ONL thickness, F (14, 160) = 7.4, P < 0.0001. Further post hoc analysis revealed a significant decrease (P < 0.0001) in homozygote infants (130.9 ± 3.6 and 40.5 ± 2.3) when compared to infant wildtype (204.3 ± 12.0 and 89.9 ± 6.5) at total foveal thickness and at foveal ONL thickness. No statistical significance was found between infant wildtype and heterozygotes. Images show a comparison of macular regions in infant wildtype, heterozygous, and homozygous primates aged 3 to 7 months. SD-OCT scans depict normal foveal appearance in wildtype (**B**) and heterozygous (**F**) primates but foveal thinning in homozygous infant (**J**). The macular area is marked with *white arrows* directing attention to macular differences among wildtype, heterozygous, and homozygous primates. Fundus autofluorescence depicting normal macular appearance in wildtype (**C**) and heterozygous (**G**) infants, but prominent foveal hyperautofluorescence is seen in homozygous infants (**K**). Color fundus shows normal macular appearance in wildtype (**D**) and heterozygous (**H**) but absent foveal light reflex in homozygous infants (**L**). Red free fundus photography showing normal foveal light reflection in wildtype (**E**) and heterozygous (**I**) but absent foveal light reflex in homozygous macaques (**M**).

light-adapted 3.0 cd•s•m^{-2} a-, b-, and flicker b-wave amplitudes were collected. After performing a 1-way ANOVA with Dunnett's analysis, we saw that when compared to wildtype infants (27.63 ± 1.7, 116.2 ± 11.2, and 96.2 ± 9.3 µV), homozygote infants had near-absent cone responses (0.01 ± 0.3, 0.1 ± 0.1, and 0.8 ± 0.5 µV, $P \leq 0.0001$). We found no statistical difference between wildtype and heterozygote (31.5 ± 1.8, 121.4 ± 9.2, and 88.4 ± 7.2 µV) infants (P = 0.1439, light-adapted 3.0 cd•s•m-2 a- and b-waves, and flicker b-waves, respectively; see Fig. 1A, Supplementary Fig. S1).

To estimate onset of cone photoreceptor structural alterations we evaluated the infant foveal retinal layer thickness from *PDE6C* wildtype (n = 5), homozygous (n = 12), and heterozygous (n = 6) rhesus macaques with SD-OCT. We took measurements at a single point at the foveal center. A 2-way ANOVA with Dunnett's multiple comparisons indicated that homozygote infant macaques had a significant reduction (P < 0.0001) in total foveal thickness (130.9 ± 3.6 µm) when compared with age-matched wildtype macaques (204.3 ± 12.0 µm, P < 0.0001). We found no statistical difference between wildtype and heterozygotes (200.8 ± 11.3 µm, P = 0.8932) as shown in Figure 2A and Supplementary Figure S2a. Similarly, homozygote macaques (40.8 ± 2.0 µm) had a significant foveal ONL thickness reduction (P < 0.0001) when compared to wildtype (89.9 ± 6.5 µm). Once again, we found no statistical difference between wildtype and heterozygotes (77.2 ± 7.9 µm, P = 0.2730; see Fig. 2A, Supplementary Fig. S2b). Thicknesses of other retinal layer thicknesses did not significantly differ between

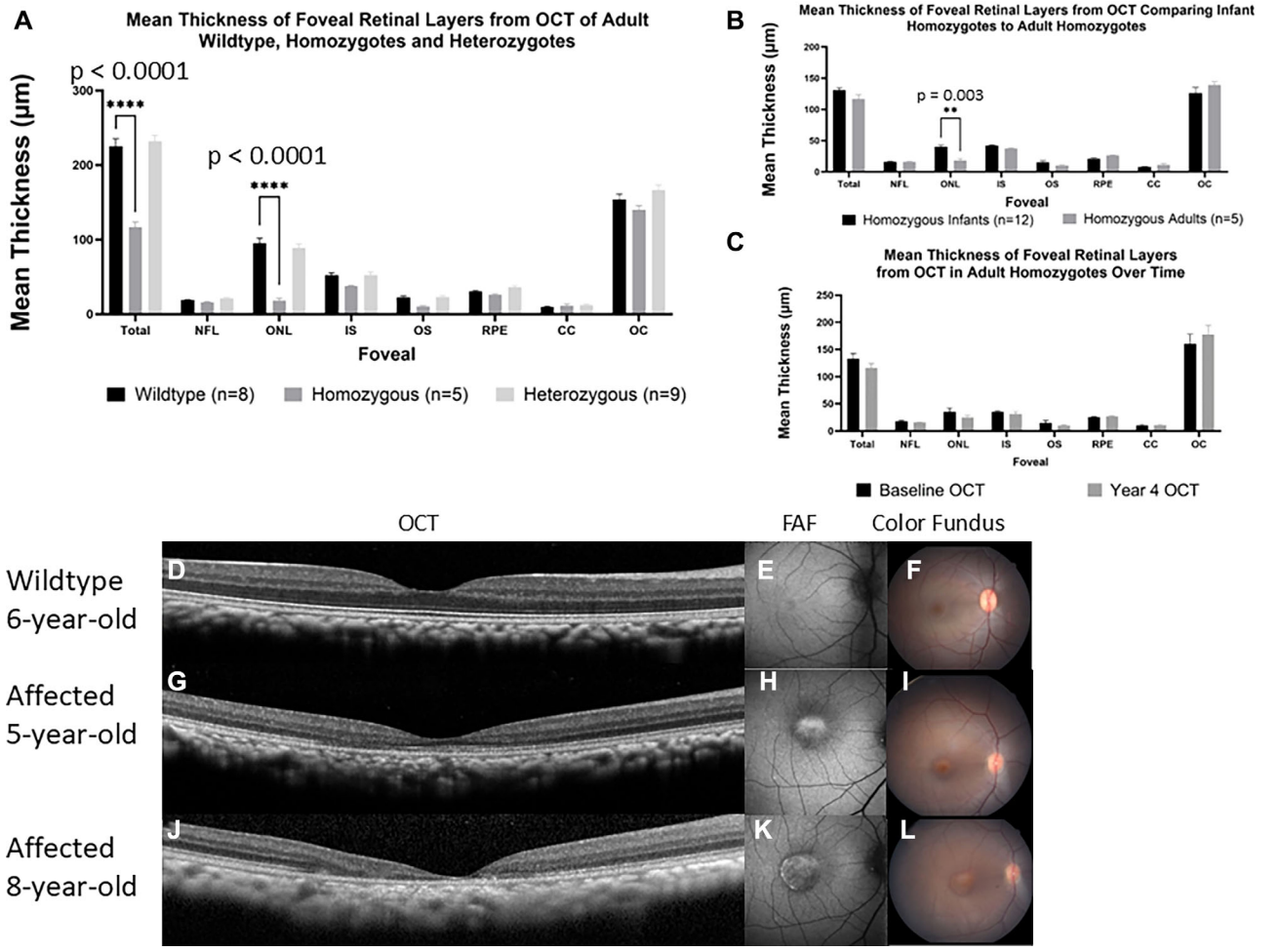

Figure 3. Foveal ONL thickness decreases from infancy to adulthood but remain stationary as an adult. (**A**) Quantification of the foveal center thickness of adult wildtype ($n = 8$), homozygous ($n = 5$), and heterozygous ($n = 9$) are presented in a bar graph as mean ± SEM. Two-way ANOVA revealed a significant interaction between genotype and retinal layer thickness at total foveal thickness and at foveal ONL thickness, $F\,(14, 152) = 19.53$, $P < 0.0001$. Further post hoc analysis revealed a significant decrease ($P < 0.0001$) in homozygote adults (116.7 ± 6.9 and 18.2 ± 3.2) when compared to adult wildtype (225.2 ± 10.0 and 95.3 ± 6.6) at total foveal thickness and at foveal ONL thickness. No statistical significance was found between adult wildtype and heterozygotes. (**B**) Comparison between mean ± SEM thickness of retinal layers from spectral domain optical coherence tomography (SD-OCT) comparing adult homozygotes ($n = 5$) to infant homozygotes ($n = 12$). Two-way ANOVA revealed a significant interaction between age and retinal layer thickness at foveal ONL thickness, $F\,(7, 120) = 3.323$, $P = 0.003$. Further post hoc analysis revealed a significant decrease ($P = 0.003$) in homozygote adults (18.2 ± 3.2) when compared to homozygote infants (40.8 ± 2.0). No statistical significance was found between adult wildtype and heterozygotes. (**C**) Comparison between the same individual homozygote adult macaques ($n = 5$) over the course of 4 years showed no significant difference in any retinal layer thickness. Data is presented as mean ± SEM thickness and statistical analysis was performed with multiple paired *t*-test. SD-OCT scans of the foveal center is shown from one 6-year-old wildtype adult (**D**) and a homozygote adult at 5 (**G**) and 8 (**J**) years of age showing macular atrophy progression. Fundus autofluorescence shows normal macular autofluorescence of a wildtype 6-year-old adult (**E**) but reveals obvious foveal hyperautofluorescence of a 5-year-old homozygote adult (**H**) that progresses as the primate ages (**K**). Fundus photography shows normal macular appearance in wildtype adults (**F**) and prominent foveal pigmentation of homozygote primate that worsens with age (**I**, **L**).

genotypes indicating that reduced total foveal thickness in homozygote infants was secondary to reduced foveal ONL thickness. Foveal thickness did not significantly differ between heterozygous and wildtype infants ($P = 0.3$; see Fig. 2A, Supplementary Table S2). Homozygous infants as young as 3 months postnatal demonstrated foveal thinning (Fig. 2J, Supplementary Figs. S2a, S2b, S2e) as well as foveal hyperautofluorescence and absent foveal light reflex (Figs. 2K, 2L, 2M) when compared to wildtype (see Figs. 2B–E) and heterozygous (see Figs. 2F–I) infant macaques.

To determine if there may be alterations in the retinal layers involving retinal cell types not in the foveal center, we performed measurements at other eccentricities within the parafoveal area 1 mm nasal and 1 mm temporal to the foveal center. Similar to the previous analyses, we used a 2-way ANOVA nasal to the fovea and another 2-way ANOVA temporal to the fovea with Dunnett's multiple comparisons where wildtype is the control group in all cases. We found that the total retinal thickness ($P < 0.0001$) and ONL ($P < 0.0001$) at the nasal measurement are significantly reduced in infant homozygote macaques (290.8 ± 4.9 and 47.8 ± 1.9) when compared to wildtype macaques (356.3 ± 19.0 and 71.6 ± 4.7), respectively. Wildtype and heterozygote macaques (356.0 ± 18.5 and 67.4 ± 3.3) had no significant difference in their total retinal thickness ($P = 0.9992$) and ONL thickness ($P = 0.4395$), respectively. Similar results

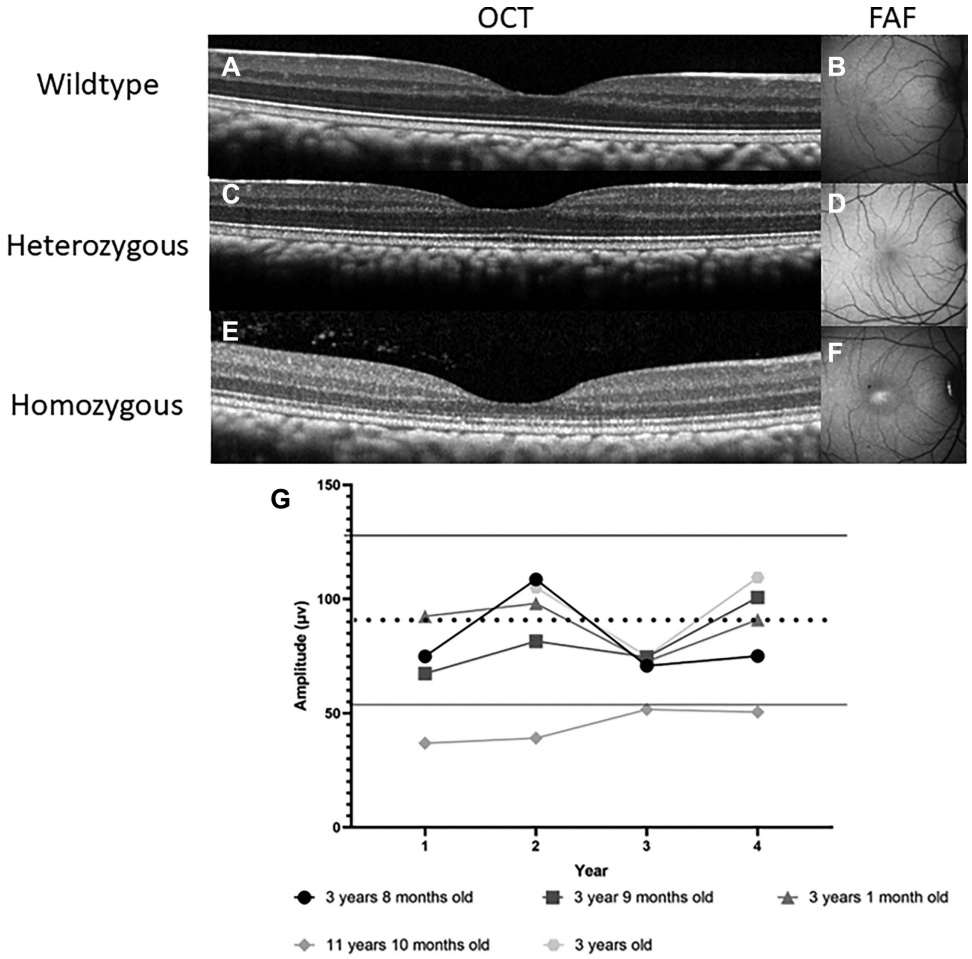

Figure 4. Adult homozygote macaques are shown to have a thinner ONL and one macaque was found to have a subnormal rod photoreceptor response. Spectral-domain optical coherence tomography (SD-OCT) images of the foveal center showing normal foveal thickness in adult wildtype (**A**) and heterozygote (**C**) but foveal ONL thinning of homozygote (**E**) animal. Fundus autofluorescence photography depicts normal macular appearance in wildtype (**B**) and heterozygote (**D**) animals but shows foveal hyperautofluorescence in homozygote animal (**F**). (**G**) Electroretinogram amplitudes (μV: microvolts) of rod a-wave from homozygous ($n = 5$) adult primates was quantified to compare the change in amplitude over the course of 4 years. Primate ages from their first year of imaging are listed next to their respective symbols. Under dark adapted conditions using a 3.0 cd•s/m^2 stimulus, the rod system was tested in 5 homozygote adults. Four out the five primates were found to be within normal macaque amplitudes and remained stable. The oldest (11-year-old) homozygote primate was found to have subnormal rod function. The *dashed line* represents the mean, and the solid line represents one SD ± from the mean of normal macaque amplitudes.

were also seen in temporal measurements where total retinal thickness ($P < 0.0001$) and ONL ($P < 0.0001$) are significantly reduced in infant homozygote macaques (273.0 ± 4.9 and 42.9 ± 1.2) when compared to wildtype macaques (340.3 ± 17.0 and 71.3 ± 5.6). Wildtype and heterozygote (343.8 ± 15.9 and 61.4 ± 4.3) primates have no significant difference of total foveal thickness ($P = 0.8550$) and ONL thickness ($P = 0.3209$), respectively (Supplementary Figs. S3a, S3b).

Evidence of Disease Progression

We first characterized retinal anatomy in adult animals to subsequently discern if there was evidence of progression in rhesus macaques with *PDE6C* disease. Foveal retinal layer thickness quantification with SD-OCT in adult primates (age = 3–16 years), using a 2-way ANOVA with Dunnett's multiple comparisons tests confirmed that homozygotes ($n = 5$) had a significant reduction ($P < 0.0001$) in total foveal thickness (116.7 ± 6.9 μm) when compared with wildtype ($n = 8$, 225.2 ± 10.0 μm) adult macaques. No significant difference was seen when wildtype and heterozygote macaques ($n = 9$, 232.0 ± 7.8 μm) were compared ($P = 0.4513$). Similarly, homozygotes (18.16 ± 3.2 μm) had a thinner ONL ($P < 0.0001$) when compared to wildtypes (95.3 ± 6.6 μm). Wildtype and heterozygotes (89.0 ± 4.9 μm) had no difference in ONL thickness ($P = 0.5030$; see Fig. 3A, Supplementary Figs. S2c–S2e).

We also measured retinal layers at the nasal and temporal area adjacent to the foveal center to assess if any other retinal layers are affected in homozygous adults. Consistent with infant results, a 2-way ANOVA with Dunnett's multiple comparisons test confirmed that adult homozygotes (261.5 ± 9.9 and 25.5 ± 3.5) had a significant reduction of both total retinal thickness ($P< 0.0001$) and of the ONL ($P < 0.0001$) nasal to the fovea when compared to wildtype (362.9 ± 12.0 and 71.0 ± 2.9). Total retinal thickness ($P = 0.1091$) and ONL thickness ($P = 0.4395$) did not significantly differ

Investigative Ophthalmology & Visual Science

between wildtype and heterozygote (375.8 ± 11.9 and 71.2 ± 2.6) primates. This was also seen temporal to the fovea where adult homozygotes (241.0 ± 10.1 and 23.3 ± 3.3) had significant reduction of both total retinal thickness ($P < 0.0001$) and of the ONL ($P < 0.0001$) when compared to wildtype (349.0 ± 12.1 and 63.5 ± 4.9). When wildtype primates were compared to heterozygote (353.6 ± 14.8, 68.1 ± 4.4) macaques, no difference was found in the total retinal thickness ($P = 0.8079$) or ONL thickness ($P = 0.8087$; see Supplementary Figs. S3c, S3d).

Heterozygote infants and adults had no significant difference in any foveal thickness measurements when compared to wildtype infant and adult primates (see Fig. 2A, Fig. 3A). Furthermore, heterozygous infant macaques (Figs. 2F–I) appear indistinguishable from wildtype infant macaques (see Figs. 2B–E) on clinical examination, color fundus images, OCT, and fundus autofluorescence (FAF) images. Heterozygous adult macaques (Figs. 4C–D) were found to be similar to wildtype adult macaques (see Figs. 4A, 4B).

To determine if the cone phenotype worsens with age, we compared retinal anatomy between infant and adult macaques. A 2-way ANOVA with the Holm-Šídák method revealed that homozygous adult macaques had a significantly lower ($P = 0.003$) foveal ONL thickness (18.2 ± 3.2 µm) when compared to homozygous infant macaques (40.8 ± 2.0 µm; see Fig. 3B). We then compared retinal anatomy of the same 5 homozygous adult macaques from their first baseline OCT examination time point and again 4 years later. We performed multiple paired *t*-tests within these five homozygous adult animals and found that, as a group, there was no significant difference in any of the retinal layer thicknesses, although there was a trend toward reduced foveal ONL (see Fig. 3C). However, one adult female homozygote macaque developed progressive macular atrophy between 5 and 8 years of age (Figs. 3G–L). When the primate was 5 years of age, the outer foveal layers were decreased and hard to discern, such as the IS and OS (see Fig. 3G). Once the primate reached 8 years of age, all of the outer retinal layers in the fovea and temporal to it were no longer distinguishable (see Fig. 3J).

We also compared retinal function between infant and adult macaques. Photopic ERGs (single flash and flicker) were performed on homozygous, heterozygous, and wildtype macaques in infancy ($n = 11$, $n = 11$, and $n = 6$, respectively) and adulthood ($n = 5$, $n = 9$, and $n = 7$, respectively). Homozygote macaques had a near zero amplitude recorded at photopic single flash and photopic flicker (see4 Fig. 1B). Heterozygous and wildtype photopic flicker amplitudes were similar at infancy and in adulthood (see Fig. 1B). However, on the single flash photopic ERG, there was a mild age-related reduction ($P = 0.0078$) in b-wave amplitude between heterozygote infant (121.4 ± 9.2 µV) and heterozygote adult (75.9 ± 5.9 µV) macaques (see Fig. 1B).

Furthermore, homozygote infants and adults had nonmeasurable photopic a-wave, b-wave, and flicker times. Wildtype (13.2 ± 0.3 ms, 26.6 ± 0.6 ms, and 24.3 ± 0.3 ms) and heterozygote primates (14.0 ± 0.4 ms, 26.7 ± 0.5 ms, and 24.9 ± 0.4 ms) had no significant difference after performing a 2-way ANOVA (see Supplementary Table S2, Supplementary Fig. S4).

Rod ERG May Decline With Age

Because the homozygotes had an absent cone response, we used the dark-adapted bright stimulus (3.0 cd•s•m^{-2}) a-wave recordings as a marker of rod photoreceptor function. We evaluated adult rod photoreceptor responses yearly for 4 years. We found that the oldest homozygote (11 years old at study initiation) presented rod photoreceptor function that fell below normal reference macaque amplitudes[16] and remained stable over the 4-year timeline. By contrast, homozygotes between 3 years and 3 years 9 months of age ($n = 4$) showed no decline in rod photoreceptor response and stayed within the reference range over the same time frame (see Fig. 4G).

Discussion

In this study, we found that the cone dysfunction and foveal structural changes are present from infancy in *PDE6C* homozygous rhesus macaques. We found no functional or morphological difference between heterozygote and control macaques at any age. Furthermore, cone cells likely slowly degenerate and macular atrophy was observed in one older case. We also found that rod photoreceptor function may be affected later in life.

Currently, there are 6 known genes that have been linked to ACHM: *CNGA3*, *CNGB3*, *GNAT2*, *ATF6*, *PDE6C*, and *PDE6H*.[4–6] In human cases with *CNGA3*, *CNGB3*, *GNAT2*, and *PDE6C*, their mean foveal thickness and mean foveal ONL thickness are significantly lower than healthy populations.[2] These results correlate to our study where *PDE6C* homozygote infant and adult primates had significantly reduced total foveal thickness and foveal ONL thickness when compared with age-matched wildtypes. Several studies have shown that subjects who have *CNGA3*, *CNGB3*, *GNAT2*, or *PDE6C*, will have some sort of disruption to the ellipsoid zone, such as disruption in the inner segment ellipsoid (ISe) or the presence of optical empty cavities at the fovea that are visible on SD-OCT.[2,11,17] These results contrast slightly with our study because no optically empty cavities were seen in *PDE6C* primates. However, one of our affected primates developed macular atrophy and over time the ellipsoid zone became disrupted. Subjects with *ATF6* achromatopsia have a different phenotype that does not appear to have foveal ONL thickness reduction when compared with healthy controls, *CNGA3*, or *CNGB3*.[18] Furthermore, in patients with deletions of exons 2 and 3 in the *ATF6* gene, OCT images revealed foveal hypoplasia and focal disruption in the ISe layer at the site of the presumed foveal pit.[19] When looking at *PDE6H* OCT images, Kohl et al. saw that all retinal layers are identifiable and continuous except the inner/outer segment (IS/OS) junction where the cone photoreceptors could not be clearly distinguished.[20]

Variants of *PDE6C* have been reported to cause both complete and incomplete ACHM and cone dystrophy[4] and the phenotype is first apparent in human infancy as photophobia, hemeralopia, and absent cone ERG amplitudes.[4,8] In a study by Varela et al., they examined 1 child heterozygous for *PDE6C*-ACHM and 1 child homozygous for *PDE6C*-ACHM, and 2 adults homozygous for *PDE6C*-ACHM mutations and found that the children had minor to no structural retinal changes and normal central foveal thickness but the adults had macular dystrophy.[14] They also found no significant differences among children and adults regarding visual acuity, color discrimination, and subjective level of visual functioning.[14] Consistent with human retinal structure, we found that infant primates as young as 3 months postnatal showed globally normal foveal architecture with

Investigative Ophthalmology & Visual Science

significantly reduced foveal thickness, and that adult animals showed clearer signs of foveal problems.[21]

Another study found that 8 adult (mean age ± SD at baseline OCT was 36 ± 8 years) individuals with *PDE6C*-ACHM (n = 7 were women, and n = 1 was a man) had no foveal hypoplasia or residual ellipsoid zone (EZ) at the foveal center.[4] One subject had absent EZ, three subjects had a hyporeflective zone, and four subjects had outer retinal atrophy.[4] Their rate of progression was similar between eyes but varied among individuals. Two younger subjects progressed at a rate faster than two older subjects and three subjects showed minimal if any change.[4] Four subjects did not have macular atrophy and the authors observed reduced foveal ONL thickness where the mean ONL thickness ± SD was 51.75 ± 6.98 um for the right eye with no further thinning over time.[4] The results from their study are similar to our results here where adult homozygote primates had no further thinning over the course of 4 years, suggesting a plateau in cone cell loss.

It is unclear whether all *PDE6C*-disease is progressive. There are studies that provide evidence for both progression and disease stability.[10–12,22] The degree of progression may depend in part on the particular mutations, genetic background, and environmental factors. In this study, we show that PDE6C-R565Q homozygous rhesus macaques have a cone disorder which worsens over time. We found that adult homozygote primates had a significant decrease in foveal ONL compared to infants suggesting that *PDE6C*-ACHM in monkeys is progressive. Additionally, we observed one homozygote 5-year-old primate develop macular atrophy. The disruption of the EZ line was apparent on SD-OCT and abnormal autofluorescence was also observed at the fovea. However, when examining SD-OCT images, we saw that the rest of our homozygote adult rhesus macaques did not have absent EZ or definite progressive autofluorescence abnormalities, even in the oldest adult animal. This individual variability is similar to what was noted in other human studies, although the subjects who had macular atrophy were older than those who did not.[4,14]

Rhesus macaques are not the only animal models of *PDE6C*-ACHM. The *cpfl1* mouse and the cone specific *pde6* zebrafish models also exist. Several studies have shown that the *cpfl1* mouse mutant is a model for fast cone photoreceptor degeneration.[23–26] The mutation (116-bp insertion) is present in the *Pde6C* gene.[23–25] Mice homozygous for the *cpfl1* mutation are reported to have a normal fundus, normal retinal structure with cone photoreceptor cell degeneration, and normal rod-mediated responses but no cone-mediated response.[26] Vacuolization in the photoreceptor layer with subsequent progressive depletion of cone photoreceptors is apparent in *cpfl1* mice as young as 3 weeks of age and progresses until few cone photoreceptors are detected in 5-month-old mice.[23] In a study comparing *rd1* and *cpfl1* mouse models, they found that cone photoreceptor cell death was associated with an accumulation of cyclic guanosine monophosphate (cGMP).[25] Two studies also found that cone degeneration progressed rapidly, peaking at around postnatal day 24.[23,25] There is a similar pattern seen in zebrafish who have a mutation in the cone-specific *pde6* gene.[27] In this animal model, the *pde6* mutation leads to the rapid degeneration of all cone photoreceptors soon after formation.[27] Additionally, they found that rods also degenerate, but only in areas that were originally rich in cone photoreceptors.[27] This finding may explain why our oldest animal had subnormal rod ERG amplitudes on the dark adapted 3.0 cd•s•m^{-2} a-wave.

Mutations in *PDE6C* cause a loss-of-function in cone-specific PDE6 which leads to elevated intracellular cGMP.[28] The buildup of cGMP and unrestrained influx of Ca^{2+} causes photoreceptor cell death.[28–30] Thinning of the foveal ONL suggests cone photoreceptor cell death.[31,32] In *cpfl* mice, AAV-mediated *Pde6C* gene delivery in very young (postnatal day 14) mice effectively restored cone function.[33] This study and others suggest that early intervention targeted to cone photoreceptors to prevent progressive cell death may be beneficial. Treatment of homozygote macaques with adeno-associated virus carrying rhesus *PDE6C* should occur in infancy to maximize therapeutic efficacy for this disease.

Acknowledgments

The authors thank Monica Motta and Michelle Ferneding and the staff at the California National Primate Research for their outstanding technical support. The authors would like to thank Andrew Blandino, PhD, for assistance with statistical analysis.

Supported by the National Institutes of Health U24 EY029904 (A.M., S.M.T., J.R., J.T.S., and R.C.), P30 EY12576, and R01 EY034123 (A.M.), R01 EY033700 (S.M.T.), and K08 EY027463 (A.M.), and generous donors. This work was also supported by the California National Primate Research Center Base Grant from the National Institutes of Health, Office of the Director, OD011107. Genotyping was conducted at the functional genomics core facility partially supported by S10OD023469 and P30 EY002520 (R.C.).

Disclosure: **M. Ardon**, None; **L. Nguyen**, None; **R. Chen**, None; **J. Rogers**, None; **T. Stout**, None; **S. Thomasy**, None; **A. Moshiri**, None

References

1. Pang J-J, Alexander J, Lei B, et al. Achromatopsia as a potential candidate for gene therapy. In Anderson RE, Hollyfield JG, LaVail MM, eds. *Retinal Degenerative Diseases*. vol. 664. New York, NY: Springer; 2010;639–646.
2. Sundaram V, Wilde C, Aboshiha J, et al. Retinal structure and function in achromatopsia: implications for gene therapy. *Ophthalmology*. 2014;121:234–245.
3. Khan NW, Wissinger B, Kohl S, Sieving PA. *CNGB3* achromatopsia with progressive loss of residual cone function and impaired rod-mediated function. *Invest Opthalmol Vis Sci*. 2007;48:3864–3871.
4. Georgiou M, Robson AG, Singh N, et al. Deep phenotyping of PDE6C-associated achromatopsia. *Invest Ophthalmol Vis Sci*. 2019;60:5112–5123.
5. Weisschuh N, Stingl K, Audo I, et al. Mutations in the gene *PDE6C* encoding the catalytic subunit of the cone photoreceptor phosphodiesterase in patients with achromatopsia. *Hum Mutat*. 2018;39:1366–1371.
6. Hirji N, Aboshiha J, Georgiou M, Bainbridge J, Michaelides M. Achromatopsia: clinical features, molecular genetics, animal models and therapeutic options. *Ophthalmic Genet*. 2018;39:149–157.
7. Grau T, Ortemyev NO, Rosenberg T, et al. Decreased catalytic activity and altered activation properties of PDE6C mutants associated with autosomal recessive achromatopsia. *Hum Mol Genet*. 2011;20:719–730.
8. Moshiri A, Chen R, Kim S, et al. A nonhuman primate model of inherited retinal disease. *J Clin Invest*. 2019;129:863–874.

9. Aboshiha J, Luong V, Cowing J, et al. Dark-adaptation functions in molecularly confirmed achromatopsia and the implications for assessment in retinal therapy trials. *Invest Opthalmol Vis Sci*. 2014;55:6340–6349.
10. Brunetti-Pierri R, Karali M, Melillo P, et al. Clinical and molecular characterization of achromatopsia patients: a longitudinal study. *Int J Mol Sci*. 2021;22:1681.
11. Thiadens AA, Somervuo V, van den Born LI, et al. Progressive loss of cones in achromatopsia: an imaging study using spectral-domain optical coherence tomography. *Invest Opthalmol Vis Sci*. 2010;51:5952–5957.
12. Tekavčič Pompe M, Vrabič N, Volk M, et al. Disease progression in CNGA3 and CNGB3 retinopathy; characteristics of Slovenian cohort and proposed OCT staging based on pooled data from 126 patients from 7 studies. *Curr Issues Mol Biol*. 2021;43:941–957.
13. Hirji N, Georgiou M, Kalitzeos A, et al. Longitudinal assessment of retinal structure in achromatopsia patients with long-term follow-up. *Invest Opthalmol Vis Sci*. 2018;59:5735–5744.
14. Daich Varela M, Ullah E, Yousaf S, Brooks BP, Hufnagel RB, Huryn LA. PDE6C: novel mutations, atypical phenotype, and differences among children and adults. *Invest Opthalmol Vis Sci*. 2020;61:1.
15. Andréasson S, Tornqvist K. Electroretinograms in patients with achromatopsia. *Acta Ophthalmol (Copenh)*. 1991;69:711–716.
16. Lin KH, Tran T, Kim S, et al. Advanced retinal imaging and ocular parameters of the rhesus macaque eye. *Transl Vis Sci Technol*. 2021;10:7.
17. Madeira C, Godinho G, Grangeia A, et al. Two novel disease-causing variants in the PDE6C gene underlying achromatopsia. *Case Rep Ophthalmol*. 2021;12:749–760.
18. Mastey RR, Georgiou M, Langlo CS, et al. Characterization of retinal structure in *ATF6*-associated achromatopsia. *Invest Opthalmol Vis Sci*. 2019;60:2631–2640.
19. Lee E-J, Chiang WCJ, Koeger H, et al. Multiexon deletion alleles of ATF6 linked to achromatopsia. *JCI Insight*. 2020;5:e136041.
20. Kohl S, Coppieters F, Meire F, et al. A nonsense mutation in PDE6H causes autosomal-recessive incomplete achromatopsia. *Am J Hum Genet*. 2012;91:527–532.
21. Jiménez-Siles L, Zamorano-Martín F, García-Lorente M, et al. A new mutation in the PDE6C gene in achromatopsia. *Eur J Ophthalmol*. 2023;33:NP133–NP137.
22. Lee H, Purohit R, Sheth V, et al. Retinal development in infants and young children with achromatopsia. *Ophthalmology*. 2015;122:2145–2147.
23. Chang B, Grau T, Dangel S, et al. A homologous genetic basis of the murine *cpfl1* mutant and human achromatopsia linked to mutations in the *PDE6C* gene. *Proc Natl Acad Sci USA*. 2009;106:19581–19586.
24. Fischer MD, Tanimoto N, Beck SC, et al. Structural and functional phenotyping in the cone-specific photoreceptor function loss 1 (cpfl1) mouse mutant – a model of cone dystrophies. *Adv Exp Med Biol*. 2010;664:593–599.
25. Trifunović D, Dengler K, Michalakis S, Zrenner E, Wissinger B, Paquet-Durand F. cGMP-dependent cone photoreceptor degeneration in the cpfl1 mouse retina. *J Comp Neurol*. 2010;518:3604–3617.
26. Chang B, Hawes NL, Hurd RE, Davisson MT, Nusinowitz S, Heckenlively JR. Retinal degeneration mutants in the mouse. *Vision Res*. 2002;42:517–525.
27. Stearns G, Evangelista M, Fadool JM, Brockerhoff SE. A mutation in the cone-specific pde6 gene causes rapid cone photoreceptor degeneration in zebrafish. *J Neurosci*. 2007;27:13866–13874.
28. Gopalakrishna KN, Boyd K, Artemyev NO. Mechanisms of mutant PDE6 proteins underlying retinal diseases. *Cell Signal*. 2017;37:74–80.
29. Doonan F, Donovan M, Cotter TG. Activation of multiple pathways during photoreceptor apoptosis in the rd mouse. *Invest Opthalmol Vis Sci*. 2005;46:3530–3580.
30. Paquet-Durand F, Beck S, Michalakis S, et al. A key role for cyclic nucleotide gated (CNG) channels in cGMP-related retinitis pigmentosa. *Hum Mol Genet*. 2011;20:941–947.
31. Lujan BJ, Roorda A, Croskrey JA, et al. Directional optical coherence tomography provides accurate outer nuclear layer and Henle fiber layer measurements. *Retina*. 2015;35:1511–1520.
32. Sadigh S, Cideciyan AV, Sumaroka A, et al. Abnormal thickening as well as thinning of the photoreceptor layer in intermediate age-related macular degeneration. *Invest Opthalmol Vis Sci*. 2013;54:1603–1612.
33. Teng Y, Stout T, Li Y. Gene augmentation therapy restores cone function in PDE6c-acciocated achromatopsia. *Invest Ophthalmol Vis Sci*. 2023;64:3830.

Investigative Ophthalmology & Visual Science